

# Physics Design of a High $\beta$ Quasi-Axisymmetric Stellarator

A. Reiman<sup>1</sup>, G. Fu<sup>1</sup>, S. Hirshman<sup>4</sup>, L. Ku<sup>1</sup>, D. Monticello<sup>1</sup>, H. Mynick<sup>1</sup>, M. Redi<sup>1</sup>, D. Spong<sup>4</sup>, M. Zarnstorff<sup>1</sup>, B. Blackwell<sup>8</sup>, A. Boozer<sup>5</sup>, A. Brooks<sup>1</sup>, W. A. Cooper<sup>2</sup>, M. Drevlak<sup>3</sup>, R. Goldston<sup>1</sup>, J. Harris<sup>8</sup>, M. Isaev<sup>9</sup>, C. Kessel<sup>1</sup>, Z. Lin<sup>1</sup>, J.F. Lyon<sup>4</sup>, P. Merkel<sup>3</sup>, M. Mikhailov<sup>9</sup>, W. Miner<sup>6</sup>, N. Nakajima<sup>7</sup>, G. Neilson<sup>1</sup>, C. Nührenberg<sup>3</sup>, M. Okamoto<sup>7</sup>, N. Pomphrey<sup>1</sup>, W. Reiersen<sup>1</sup>, R. Sanchez<sup>4</sup>, J. Schmidt<sup>1</sup>, A. Subbotin<sup>9</sup>, P. Valanju<sup>6</sup>, K. Y. Watanabe<sup>7</sup>, R. White<sup>1</sup>

<sup>1</sup>*Princeton Plasma Physics Laboratory, Princeton NJ 08543, USA*

<sup>2</sup>*CRPP-PPB, CH-1015 Lausanne, Switzerland*

<sup>3</sup>*IPP-Euratom Association, D-17491 Greifswald, Germany*

<sup>4</sup>*Oak Ridge National Laboratory, Oak Ridge, Tennessee 37831-8070, USA*

<sup>5</sup>*Dept. of Applied Physics, Columbia University, New York, NY 10027, USA*

<sup>6</sup>*University of Texas at Austin, Austin, TX 78712-1081, USA*

<sup>7</sup>*National Institute for Fusion Science, Nagoya, Japan*

<sup>8</sup>*Plasma Research Laboratory, Australian National University, Canberra, Australia*

<sup>9</sup>*Kurchatov Institute, Moscow, Russia*

## Abstract

Key physics issues in the design of a high  $\beta$  quasi-axisymmetric stellarator configuration are discussed. The goal of the design study is a compact stellarator configuration with aspect ratio comparable to that of tokamaks and good transport and stability properties. Quasi-axisymmetry has been used to provide good drift trajectories. Ballooning stabilization has been accomplished by strong axisymmetric shaping, yielding a stellarator configuration whose core is in the second stability regime for ballooning modes. A combination of externally generated shear and nonaxisymmetric corrugation of the plasma boundary provides stability to external kink modes even in the absence of a conducting wall. The resulting configuration is also found to be robustly stable to vertical modes, increasing the freedom to do axisymmetric shaping. Stability to neoclassical tearing modes is conferred by a monotonically increasing  $\iota$  profile. A gyrokinetic  $\delta f$  code has been used to confirm the adequacy of the neoclassical confinement. Neutral beam losses have been evaluated with Monte Carlo codes.

## 1. Introduction

We have been pursuing the design of a compact stellarator configuration with aspect ratio comparable to that of tokamaks ( $R/\langle a \rangle \approx 3.5$ ) and good transport and stability properties. To provide good drift trajectories, we have focused on configurations that are close to quasi-axisymmetric (QA).[1, 2] This paper discusses key physics issues that have been addressed in our study.

The QA configurations being studied have drift trajectories similar to those of tokamaks, aspect ratios comparable to those of tokamaks, and bootstrap current as well as  $n = 0$  components of ellipticity and triangularity comparable to that of advanced tokamaks. They therefore can be considered to be hybrids between drift-optimized stellarators and advanced tokamaks. Relative to unoptimized stellarators, they have improved predicted neoclassical confinement. They have a much smaller aspect ratio than the drift-optimized stellarators under construction. Strong axisymmetric components of shaping provide good ballooning stability properties at the lower aspect ratio. The bootstrap current, large relative to that of other drift-optimized stellarators, is used to advantage in suppressing magnetic islands and providing a substantial fraction

of the rotational transform. An experimental study of the potential benefits and disadvantages of bootstrap currents would be a key focus of a proposed QA stellarator experiment.

Relative to advanced tokamaks, QA configurations have the potential advantage that the externally generated transform reduces or eliminates the need for rf current drive and provides control over MHD stability properties. Unlike the tokamak, it is possible to have a monotonically increasing  $\iota$  profile (monotonically decreasing  $q$  profile), avoiding problems associated with MHD stability at the shear reversal layer, and conferring stability to neoclassical tearing modes across the entire cross section. A combination of externally generated shear and nonaxisymmetric corrugation of the plasma boundary provides stability to external kink modes even in the absence of a conducting wall. The resulting configuration is found to be robustly stable to vertical modes. Experiments on hybrid tokamak-stellarator configurations on W7A and CLEO found that even a modest level of externally generated transform was sufficient to suppress disruptions.[3, 4].

Section 2 of this paper describes an approximately quasi-axisymmetric configuration that we call Configuration C82, and discusses some of its properties. Section 3 discusses the issues of kink, vertical, and ballooning stability. Section 4 discusses neoclassical confinement of thermal and energetic particles.

## 2. An Approximately Quasi-Axisymmetric Configuration

Figure 1 shows the plasma boundary of an approximately quasi-axisymmetric, three-period configuration that we call Configuration C82. The choice of aspect ratio ( $R/\langle a \rangle \approx 3.4$ ) has been constrained by the desire to fit the configuration inside the PBX-M tokamak toroidal field (TF) coils. We envision constructing a device that would reuse the PBX TF coils to produce the main component of the toroidal field, and would have an additional set of saddle coils inside the TF coils to produce the three-dimensional field components. Configuration C82 is the most recent of a set of configurations that have been generated through a design procedure that uses an optimizer to adjust the values of about 40 parameters specifying the shape of the plasma boundary to target desired configuration properties.

The configuration optimization is performed using a Levenberg-Marquardt scheme to minimize a target function,  $\chi^2$ , which is a sum of squares of desired targets.[5] Targets incorporated in the optimizer include: a measure of quasi-axisymmetry (the sum of the squares of the non-axisymmetric Fourier components of  $B$  in Boozer coordinates, with an adjustable weighting of contributions from different flux surfaces); a measure of secondary ripple wells along the field lines[6]; the eigenvalue of the most unstable external kink mode; ballooning eigenvalues; the deviation of major radii of inner and outer boundaries from those prescribed by the PBX geometry; the deviation of the rotational transform from prescribed values on one or two flux surfaces. Configurational properties (MHD equilibria) are completely determined by the current and pressure profiles, as well as the plasma boundary, which is represented as a finite sum of Fourier harmonics for  $R$  and  $Z$ . Varying these as independent variables in the optimizer allows us to seek stellarator configurations which minimize  $\chi^2$  and thereby approach a state in which the various criteria are satisfied as well as possible. The VMEC code[7] is used to calculate the MHD equilibria needed to evaluate the physics targets for arbitrary values of the independent variables. The attainment of an optimized state has been accelerated by introducing a condensed spectrum for the boundary. For Configuration C82, 6 poloidal modes and 3 toroidal modes were used in the plasma boundary description, resulting in 39 independent

variables adjusted by the optimizer. The optimization process typically used 94 modes and 33 radial grid surfaces for its VMEC calculations. Kink eigenvalue calculations in the optimizer use the TERPSICHORE code.[8]

A tokamak equilibrium from the ARIES reactor study[9] was used as the starting point of the optimization procedure. This starting point has an advantage that it has good ballooning stability properties. Also, we initially retain the bootstrap-like current profile as well as the pressure profile of the ARIES equilibrium. The  $\beta$  limit for the ARIES configuration is 4.5%, and we fix  $\beta$  at 4% for the purposes of our optimization study. We assume a broader density profile than that used in the ARIES study, and the magnitude of the bootstrap current is consequently reduced. The pressure and current profiles are held fixed in the optimization process, along with the total toroidal flux. The initially axisymmetric equilibrium is of course quasi-axisymmetric, and we use the optimizer to maintain approximate quasi-axisymmetry as we deform the boundary to introduce an externally generated rotational transform. In order to avoid difficulties associated with local optima in the optimizer target function, the modification of the ARIES equilibrium to produce Configuration C82 was done in four stages. In the initial stage, the value of  $\iota$  at the magnetic axis and the plasma edge were targeted, as well as the quasi-axisymmetry. By this means, an approximately uniform external transform was added to the axisymmetric configuration until, on average, it accounted for about 30% of the total. Only the  $n \neq 0$  terms were varied at this stage. The weight placed on the ripple measure in the target function was adjusted to reduce the magnitude of individual Fourier components of  $B$  to less than a few percent. The resulting  $\iota$  profile was non-monotonic, with a region near the edge where  $\iota' < 0$ . In the second stage of the optimization procedure, the value of  $\iota$  was constrained at a point in the plasma interior and at the plasma edge, and the value at the edge was raised to make the profile monotonic. The value of  $\iota$  at the axis was not constrained during this second stage of optimization, and it decreased somewhat. The non-axisymmetric magnetic field components were also further reduced at this stage. For the third stage of the procedure, the kink stabilization was turned on in the optimizer target function, retaining the constraints on quasi-axisymmetry and on the value of  $\iota$  at the edge. The  $n = 0$  terms now were allowed to vary (with the aspect ratio being constrained). The reduction of secondary ripple wells was also done at this stage. Finally, after kink stabilization, we find that the ballooning beta limit near the edge has been lowered, and is now exceeded locally by the pressure gradient in a narrow region. This requires a local reduction in  $p'$  in that region. (The initially adopted ARIES profile has a relatively large pressure gradient near the edge.) The final pressure profile is shown in Figure 2. The coordinate  $s$  is the toroidal flux normalized to its value at the boundary.

The sign of the shear in Configuration C82 has been chosen such that the perturbed bootstrap currents suppress magnetic islands. This stabilizing effect is the inverse of the neoclassical tearing instability that has been seen in tokamak experiments. The rotational transform profile of Configuration C82 is shown in Figure 3. It ranges from about 0.25 on the axis to about 0.47 at the edge. Also shown is the vacuum transform generated by the three-dimensional shaping alone. In the absence of this externally generated transform,  $\iota$  would be decreasing in a region outside the current density peak. The externally generated transform allows us to generate a monotonically increasing  $\iota$ . In tokamak parlance,  $q' < 0$  ( $\iota' > 0$ ) is known as “reverse shear”. Reversed shear tokamaks have a shear reversal layer which tends to be associated with MHD stability problems, and outside of which neoclassical tearing modes are unstable.

Figure 4 shows the nonaxisymmetric Fourier components of  $B$  in Boozer coordinates, as a function of the radial coordinate, for Configuration C82. In the quasi-axisymmetric limit, these

Fourier modes would vanish. In our design process, we have used an optimizer to suppress these mode amplitudes. The boundary prescription of Configuration C82 has an  $m=2, n=1$  Fourier mode of amplitude 0.126. This term helps to produce the desired externally generated shear. Its amplitude may be compared with that of the  $m=2, n=1$  Fourier component of  $B$  (the largest nonaxisymmetric component), which is only 0.7% at  $s=0.5$  (relative to the  $m = 0, n = 0$  component), rising to 3.5% at the edge.

In the remainder of this paper we discuss some key physics issues in more detail. Section 3 discusses ideal MHD stability issues. Section 4 discusses confinement issues.

### 3. Ideal MHD Stability

As discussed in the previous section, the sign of  $\iota'$  in Configuration C82 confers stability to neoclassical tearing modes. In this section we discuss ballooning, kink and vertical stability. These three issues are not independent. We use a combination of externally generated shear and an appropriate corrugation of the plasma boundary to stabilize external kink modes. We have found that the resulting configurations are also robustly stable to vertical modes. The vertical stabilization, in turn, extends our freedom to use axisymmetric shaping to stabilize ballooning modes. The stability of ballooning, external kink, and vertical modes has been calculated using the TERPSICHORE[8] suite of codes. More details on the kink and vertical stability calculations will be reported in [15]. The CAS3D code has also been used for benchmarking of kink and vertical stability calculations, and to extend kink and vertical stability calculations to the case with the wall at infinity.[16, 17]

As previously reported[10, 11], we have found that ballooning modes can be stabilized in quasi-axisymmetric stellarators by appropriate axisymmetric shaping. The resulting strong axisymmetric component of shaping is a unique feature of our configurations relative to other stellarators, and is visible in Fig. 1. (Note that the average of the ellipticity and triangularity as a function of the toroidal angle does not vanish.) The ARIES tokamak equilibrium that serves as the starting point for the design procedure provides initial  $n = 0$  components of shaping that are strongly stabilizing for ballooning.

The ARIES tokamak equilibrium that serves as our starting point for the design of Configuration C82 requires a conducting wall at  $1.3a$ , where  $a$  is the minor radius, to stabilize the external kink mode. The external kink has been stabilized in Configuration C82 with the wall at infinity. To accomplish this, we have used a combination of externally generated shear and a three-dimensional corrugation of the boundary with little associated shear.

The potential use of externally generated shear to stabilize kink modes was suggested in several early papers.[12, 13] Our calculations confirm that the external kink in our quasi-axisymmetric configurations can be stabilized by this method.[14] However, we find that when externally generated shear alone is used to stabilize the kink this forces the value of  $\iota$  in the plasma interior to undesirably low values. This is particularly an issue for a reverse shear configuration of the size we could like to construct, where the axisymmetric neoclassical confinement time does not exceed the total confinement time by a large margin, so that a reduction in the total poloidal flux poses confinement problems. The development of a second kink stabilization scheme to augment the effect of the externally generated shear has therefore been key in allowing us to generate attractive kink stable configurations. The second method of stabilization employs a three-dimensional corrugation of the plasma boundary with little associated shear. The corrugation is generated using the optimizer, with the kink growth rate calculated

by TERPSICHORE incorporated in the target function. The optimizer adjusts the shape of the plasma boundary to suppress the kink.

For calculating global ideal MHD stability, the TERPSICHORE code uses finite elements in the radial direction and Fourier decomposition in the poloidal and toroidal angles. For our kink calculations, the typical numerical resolutions used are 48 radial grid surfaces, 264 equilibrium Fourier modes in Boozer coordinates and 91 stability Fourier modes. Systematic convergence studies show that this resolution is sufficient for the accurate prediction of the beta limit due to external kink modes. Up to 96 radial grid surfaces and 131 stability Fourier modes have been used.

With the ARIES pressure and current profiles, as described in Section 2, and in the absence of a conducting wall, Configuration C82 is marginally stable to external kink modes at  $\beta \approx 3.9\%$ . Figure 5 shows the dependence of the kink stability on the magnitude of the current. The configuration becomes increasingly stable to the external kink at lower current, and less stable at higher current. This is in contrast to the conventional tokamak, in which the kink  $\beta$  limit increases with increasing current. This can be understood in terms of the shear. In our configuration, the externally generated shear is opposing that due to the current near the edge. Increasing the current decreases the net shear near the edge. In a conventional tokamak equilibrium, on the other hand, the shear increases with increasing current. When the plasma current in Configuration C82 is sufficiently large, an  $\iota = .5$  surface moves into the plasma, and the configuration becomes unstable to a current driven mode at zero  $\beta$ , as can be seen in Figure 5.

The “vertical instability” in our configuration is nonaxisymmetric, unlike that in a tokamak, because of the mode coupling through the nonaxisymmetric equilibrium Fourier modes. We distinguish this type of instability from the external kink mode by its preservation of the periodicity of the equilibrium. Kink modes, in contrast, preserve the stellarator symmetry, but not the periodicity. The two types of modes do not couple in  $\delta W$ , so that their stability can be calculated independently.

The vertical mode is calculated to be stable in Configuration C82 at the reference  $\beta$  value of 3.9% with the wall at infinity. A tokamak having the same  $n = 0$  components of boundary shape is unstable. We interpret the stabilization as due to the nonaxisymmetric shaping. To study this effect, the vertical stability has been calculated for a sequence of zero  $\beta$  equilibria interpolating between the tokamak and Configuration C82. The  $n \neq 0$  components of the shape are linearly interpolated between the tokamak (zero amplitude) and their full value in Configuration C82. These calculations have been done with a wall at  $4.5a$ , where we believe it has virtually no effect on stability. The results are shown in Figure 6. About 60% of the three-dimensional shaping is adequate to stabilize the vertical mode. Finite  $\beta$  effects are found to be stabilizing. We conclude that the vertical mode is robustly stable.

The robust stability of the vertical mode allows us to further increase the elongation of our configuration. This provides additional flexibility in shaping the configuration to maintain ballooning stability. The potential usefulness of this is being explored.

The corrugation introduced to stabilize the kink mode causes a deterioration in the ballooning stability near the edge of the plasma. As described in Section 2, this requires a modest reduction of  $p'$  in the region  $0.8 < s < 0.9$  relative to the initially adopted ARIES profile in order to retain ballooning stability in this region. The resulting pressure profile is shown in Figure 2, corresponding to  $\beta = 3.8\%$ . The ballooning eigenvalues for this pressure profile are plotted in Figure 7 as a function of the radial coordinate. In the narrow region near the edge where the pressure profile has been modified, the ballooning eigenvalues approach marginal stability.

Away from this region, the ballooning mode is robustly stable.

In the core region ( $s < .3$ ), it is found that Configuration C82 is in the second stability regime for ballooning. That is, the ballooning eigenvalues become more stable when the pressure gradient in this region is increased. Peaking the pressure profile raises the ballooning  $\beta$  limit, as well as the kink  $\beta$  limit. The  $\beta$  limits of peaked pressure profiles are under study.

## 4. Neoclassical Confinement

Our numerically generated configurations are only approximately quasi-axisymmetric. In designing the configurations, it is necessary to monitor the neoclassical transport to confirm that the degree of quasi-axisymmetry is adequate. In this section we discuss calculations of neoclassical confinement of thermal particles and of neutral beams. The parameters are chosen to be appropriate for a device constructed in the PBX facility,  $R \approx 1.45$  m.

Thermal neoclassical transport evaluations have been done using the GTC code[18] running on a Cray T3E computer. GTC can do both full- $f$  and  $\delta f$  calculations in general toroidal geometry, and can run in either turbulence mode (self-consistent electrostatic fluctuations computed) or neoclassical mode (only specified magnetic and electrical fields), with like-particle collisions for ions, and like-particle plus electron-ion collisions for electrons. Calculations for NCSX thus far have used only the neoclassical mode.

The simulations used for these assessments of thermal transport used  $40 \times 10^3$  Deuterium ions, loaded according to temperature and density profiles drawn from the PBX database, with  $T_{i0} = 2.14$  keV,  $n_{e0} = 0.67 \times 10^{14}$ , and  $B=1.26$  Tesla. A model ambipolar potential  $\Phi$  is used, given by  $e\Phi/T_{i0} = \alpha\psi/\psi_{\text{edge}}$ , with  $2\pi\psi$  the toroidal flux, and  $\alpha$  an adjustable amplitude. These runs used  $\alpha = 1$ , hence  $e\Phi \approx T_i$ . GTC was run in neoclassical, full- $f$  mode, and the confinement time  $\tau_E$  computed from  $\tau_E(r) = W(r)/[-d_t W(r) + S_E(r)]$ , with  $W(r)$  the ion energy contained inside flux surface  $r$ , and  $S_E(r)$  the energy source/sink, computed from the energy exchange of the test ions off the fixed-profile background.

At  $r = a$  ( $\psi = \psi_{\text{edge}}$ ), we find  $\tau_{Ei} = 16.9$  msec for Configuration C82. Since the electron heat loss channel is negligible, the neoclassical energy confinement time is  $\tau_E^{nc} \approx (1 + W_e/W_i)\tau_{Ei}^{nc}$ . For  $Z_{\text{eff}} = 2$ , this gives  $\tau_E^{nc} \approx 2.3\tau_{Ei}^{nc} \approx 39$  ms. For these parameters,  $\tau_{\text{ISS}} \approx 7.6$  msec. An enhancement factor of 2.3 would give a confinement time of 17.5 ms. This is still well below the neoclassical confinement time, so the neoclassical losses are predicted to be sufficiently small to not have a significant deleterious effect on the energy confinement.

Neutral beam heating efficiency has been calculated by following a collection of simulation particles through several slowing-down times with the DELTA5D code[19]. These particles are initially distributed in space according to a deposition profile calculated by TRANSP[20] for an equivalent axisymmetric configuration; the initial pitch angle distribution is determined based on the ratio of the tangency radius to the birth major radius (pencil beam approximation). The Hamiltonian guiding center beam particle orbits are then followed in the presence of collisions with electrons and two background ion species (a main ion and one impurity component). As the beam ions slow down to  $3/2kT_{\text{ion}}$  with  $T_{\text{ion}}$  the background field ion temperature, they are removed from the fast ion distribution and counted as part of the field plasma. Beam heating efficiencies are calculated by recording the losses of particles and energy out of the outer magnetic flux surface that occur during the slowing-down process. The DELTA5D code runs groups of beam particles on different processors in parallel on the Cray T3E using the MPI language for inter-processor communication. A variety of diagnostics of the escaping particles, such as

pitch angle, energy and particle lifetime distributions, are retained to aid in understanding the loss mechanisms. These generally show a prompt loss peak at the beam injection energy and pitch angle, followed by a more gradual loss centered around  $v_{\parallel}/v = 0$  and at around 1/5 of the injection energy as the beam particles scatter onto trapped orbits. We also have made studies of the dependence of these losses on the magnetic field and find non-monotonic behavior in beam energy losses with increasing magnetic field strength. This type of behavior is to be expected with the presence of stochastic loss regions. Contours of the longitudinal adiabatic invariant  $J$  indicate that such loss regions can be present for barely passing particles near the plasma edge.

This model has been applied to the calculation of neutral beam energy losses for the c82 configuration, with the background plasma taken to have a central electron density of  $6.5 \times 10^{13} \text{ cm}^{-3}$ , and central temperatures of 1.9 keV for the ions, and 2.1 keV for the electrons. The background impurity species was oxygen ( $Z = 8$ , mass/proton mass = 16) with  $n_{\text{impurity}}/n_{\text{electron}} = 0.014$  leading to a  $Z_{\text{eff}}$  of 1.8. The beam consisted of 50 keV hydrogen ions injected on the midplane at  $\theta = 0$ ,  $\phi = 0$ . This resulted in saturated (over several slowing-down times) beam energy losses of 34% for  $\langle B_0 \rangle = 1\text{T}$  and 28% for  $\langle B_0 \rangle = 1.5\text{T}$ .

Energetic ion losses have also been calculated using the ORBITMN code, a modification of the ORBIT code[21] which is capable of handling three-dimensional equilibria. Simulations of  $\alpha$  particle confinement using the ORBIT code show good agreement with detailed experimental measurements on TFTR.[22] The predictions of ORBITMN are consistent with those of DELTA5D.

## 5. Conclusions

The design of an attractive quasi-axisymmetric stellarator has required the development of novel techniques for stabilizing ballooning and kink modes. Ballooning modes have been stabilized through axisymmetric shaping, not previously applied to stellarators. This results in a configuration whose core is in the second stability regime for ballooning. Kink modes have been stabilized, without a conducting wall, through a combination of externally generated shear and a three-dimensional corrugation of the boundary. The resulting configuration is also robustly stable to vertical modes. The solution of these problems opens up a promising new region of configuration design space. MHD stabilized quasi-axisymmetric stellarators combine some of the most attractive features of drift-optimized stellarators and advanced tokamaks.

The confinement predictions of Section 4 suggest that an  $R = 1.45 \text{ m}$  device based on the c82 configuration would require about 5.5 MW of neutral beam power to access 4%  $\beta$  with  $B = 1.2 \text{ T}$ ,  $n = 10^{20} \text{ m}^{-3}$ ,  $T_0 = 1.4 \text{ keV}$ . The PBX facility has 6 MW of neutral beam power available. Such a device would therefore be capable of testing the novel schemes for stabilizing ballooning, kink, and vertical modes described in Section 3. The experiment would more generally provide information on MHD stability, disruption immunity, and confinement in a compact quasi-axisymmetric stellarator operating near the  $\beta$  limit, including the potentially stabilizing effects of bootstrap currents on magnetic islands.

## Acknowledgments

This research was partially sponsored by the US Department of Energy under contract No. DE-AC02-76-CHO-3073, by the Fonds National Suisse de la Recherche Scientifique and by Euratom.

## References

- [1] J. Nührenberg, W. Lotz, and S. Gori, in *Theory of Fusion Plasmas*, E. Sindoni, F. Troyon and J. Vaclavik eds., SIF, Bologna, 1994
- [2] P.R. Garabedian, *Phys. Plasmas* **3**, 2483 (1996).
- [3] W VII-A Team, *Nucl. Fusion* **20**, 1093 (1980).
- [4] D. C. Robinson and T. N. Todd, *Phys. Rev. Letters* **48**, 1359 (1982).
- [5] D. A. Spong, S. P. Hirshman, J. C. Whitson, et. al., *Phys. Plasmas* **5**, 1752 (1998)
- [6] M. Yu. Isaev, M. I. Mikhailov, D. A. Monticello, H. E. Mynick, A. A. Subbotin, L. P. Ku , A. H. Reiman, accepted for publication in *Phys. Plasmas*.
- [7] S. P Hirshman, W. I. van Rij, and P. Merkel, *Comput. Phys. Commun.* **43**, 143 (1986).
- [8] D.V. Anderson, A. Cooper, U. Schwenn and R. Gruber, *Linear MHD Stability Analysis of Toroidal 3D equilibria with TERPSICHORE* in “Theory of Fusion Plasmas,” J. Vaclavik, F. Troyon and E. Sindoni eds. (Soc. Ital. Fisica – Editrice Compositori, Bologna, 1988) pp. 93–102
- [9] S.C. Jardin, C. E. Kessel, C.G. Bathke, D.A. Ehst, T.K. Mau, F. Najmabadi, T.W. Petrie, ”Physics Basis for a Reversed Shear Tokamak Power Plant”, *Fusion Engr. and Design*, vol. 38, (1997), 27.
- [10] A. Reiman, R. Goldston, L. Ku, D. Monticello, H. Mynick, G. Neilson, M. Zarnstorff, I. Zatz, W. Cooper, and A. Boozer, *J. Plasma Fusion Res. SERIES* **1**, 429 (1998).
- [11] A. Reiman, L. Ku, D. Monticello, H. Mynick, and the NCSX Configuration Design Team, 1999 Fusion Energy Proc. 17th Int. Conf. (Yokohama, 1998) (Vienna: IAEA), paper IAEA-F1-CN-69/ICP/06.
- [12] V. V. Drozdov, M. Yu. Isaev, M. I. Mikhailov, V. D. Pustovitov, and V. D. Shafranov, in *Plasma Physics and Controlled Nuclear Fusion Research 1988* (Proc. 12th Int. Conf. Nice, 1988), Vol. 2, IAEA, Vienna (1989) 611.
- [13] J. L. Johnson et al, *Phys. Fluids* **1**, 281 (1958); R. M. Sinclair et al, *Phys. Fluids* **8**, 118 (1965); K. Matsuoka et al, *Nuclear Fusion* **17**, 1123 (1977).
- [14] G. Fu, L. Ku, N. Pomphrey, M. Redi, C. Kessel, D. Monticello, A. Reiman, M. Hughes, W. Cooper and C. Nuehrenberg, 1999 Fusion Energy Proc. 17th Int. Conf. (Yokohama, 1998) (Vienna: IAEA)
- [15] G.Y. Fu et al, Ideal MHD stability in high beta current-carrying quasi-axisymmetric stellarators, in preparation.
- [16] C. Nuehrenberg, *Phys. Plas.* **3**, 2401 (1996). C. Schwab, *Phys. Fluids B5*, 3195 (1993).
- [17] M. H. Redi, et al ”Vertical and Kink Mode Stability Calculations for Current Carrying Quasixial Stellarators”, Paper P4.085, this conference.

- [18] Z. Lin, T.S. Hahm, W.W. Lee, W.M. Tang, R.B. White, *Science* **281**, 1835 (1998).
- [19] D.A. Spong, S.P. Hirshman, D.B. Batchelor, J.F. Lyon, "Plasma Transport and Energetic Particle Confinement Studies in Low Aspect Ratio Quasi-Omnigenous (QO) Stellarators" Bulletin of the American Physical Society, Abstract KP01.45, March 20-26, 1999, Atlanta, GA.
- [20] R.J. Hawryluk in Physics of Plasmas Close to Thermonuclear Conditions, ed. by B. Coppi, et al., (CEC, Brussels, 1980), Vol. 1, p. 19.; R.J. Goldston et al., *J. Comp. Phys.* 43 (1981) 61.
- [21] R. White and M. Chance, *Phys Fluids* 25, 575 (1982); R. White, *Phys Fluids B* 2, 575 (1990).
- [22] "Neoclassical Simulations of Fusion Alpha Particles in Pellet Charge Exchange Experiments on the Tokamak Fusion Test Reactor", M. H. Redi S. H. Batha, R. V. Budny, D. S. Darrow, F. M. Levinton, D. C. McCune, S. S. Medley, M. P. Petrov, S. vonGoeler, R. B. White, M. C. Zarnstorff, S. J. Zweben, *Phys. Plas.*, in press (1999).
- [23] "Energetic Particle Confinement in Compact Quasixial Stellarators" M. H. Redi, H. E. Mynick, M. Suewattana, R. B. White, M. C. Zarnstorff, *Phys. Plas.*, in press (1999).

## Figures

Fig. 1 Plasma boundary of Configuration C82.

Fig. 2 Pressure profile. The coordinate  $s$  is the toroidal flux normalized to its value at the boundary.

Fig. 3 Rotational transform profile of Configuration C82.

Fig. 4 Largest nonaxisymmetric Fourier coefficients of  $B$  for Configuration C82, normalized to  $n = 0, m = 0$  Fourier component.

Fig. 5 Kink stability of Configuration C82 with varying  $\beta$  and current. Open circles correspond to stable equilibria, filled circles to unstable equilibria.

Fig. 6 Vertical stability eigenvalues calculated by TERPSICHORE for a sequence of equilibria interpolating between Configuration C82 and a corresponding tokamak.

Fig. 7 Ballooning eigenvalues as a function of radial coordinate for the modified pressure profile.

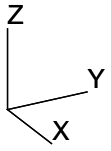
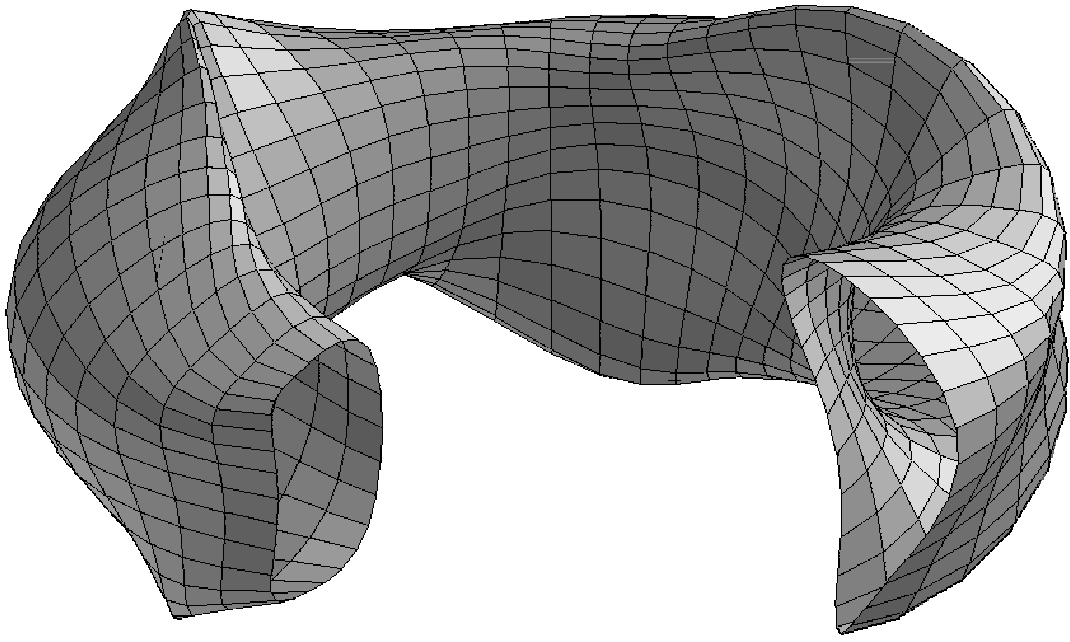


Figure 1:

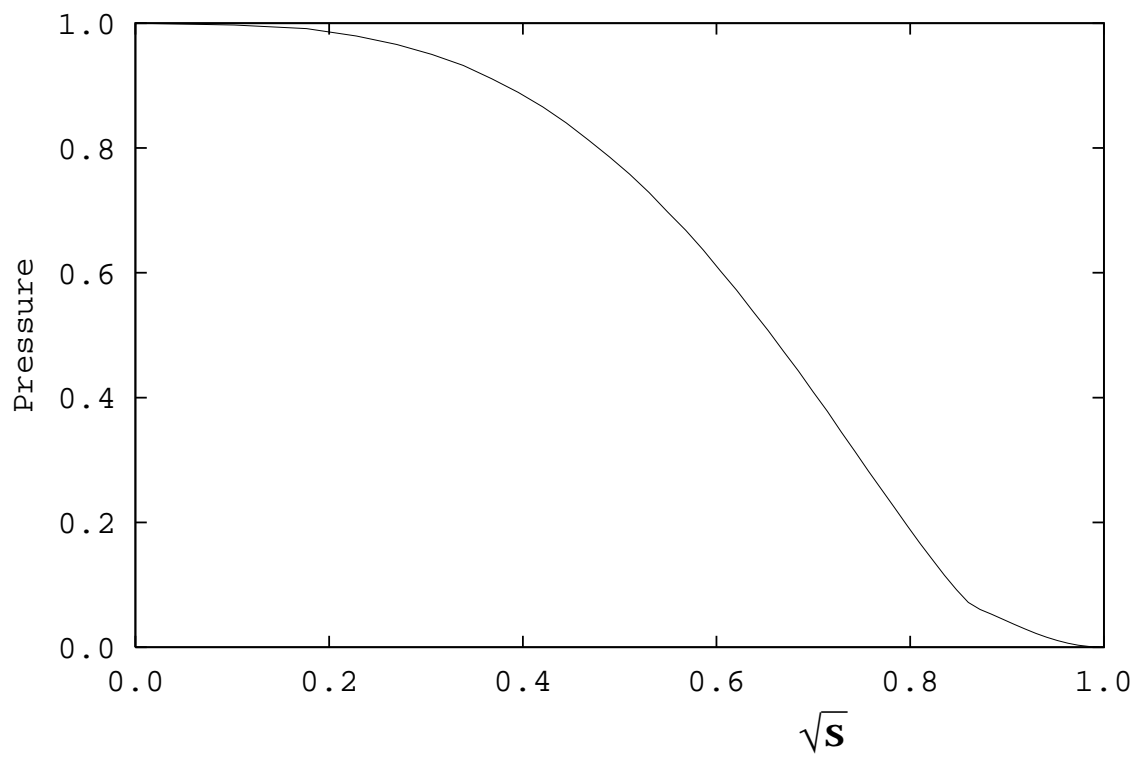


Figure 2:

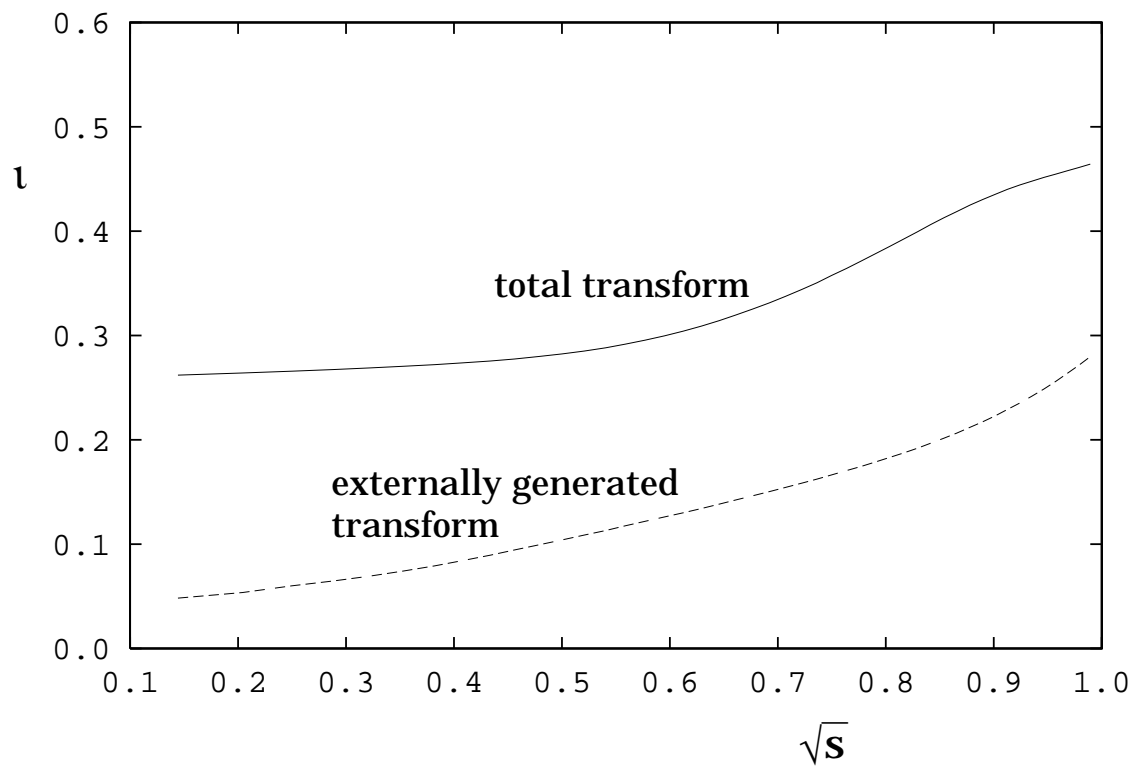


Figure 3:

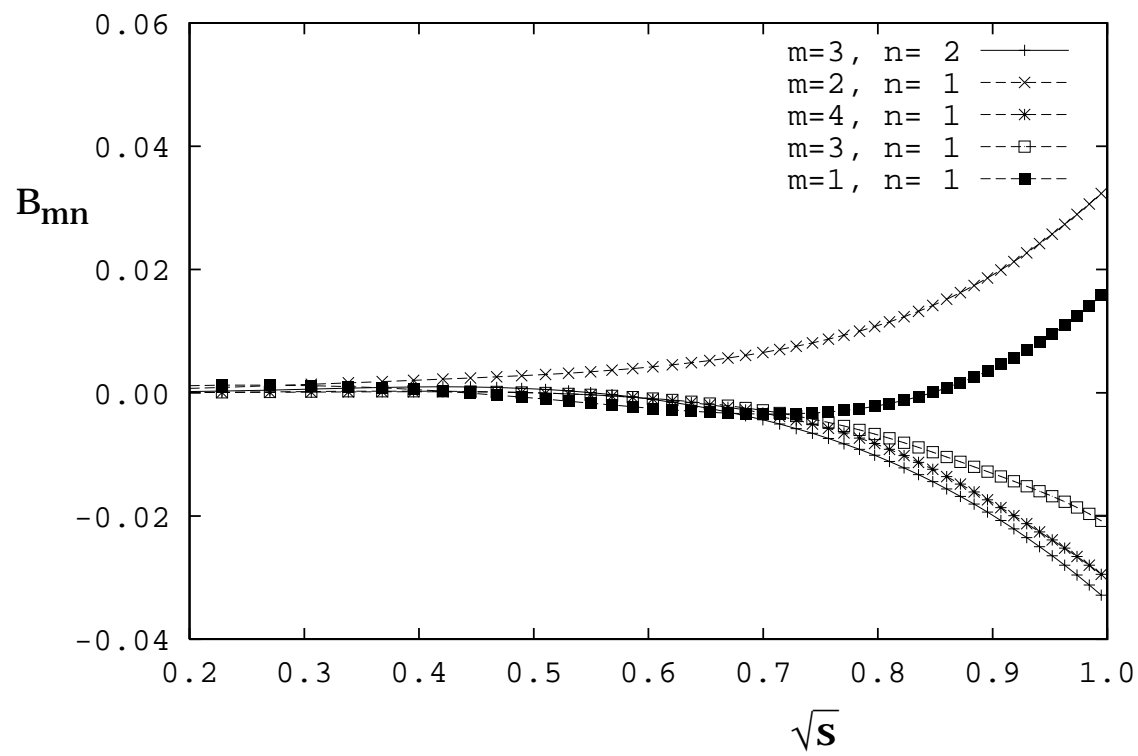


Figure 4:

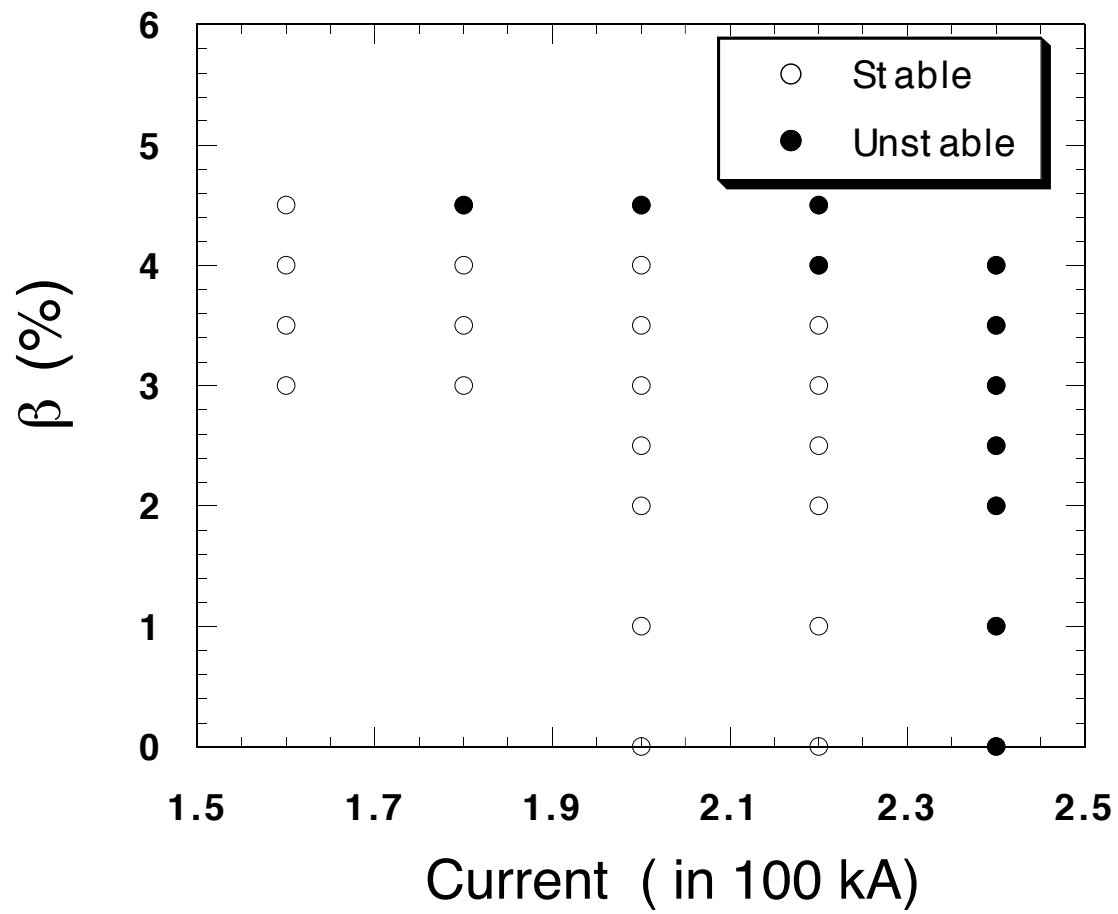


Figure 5:

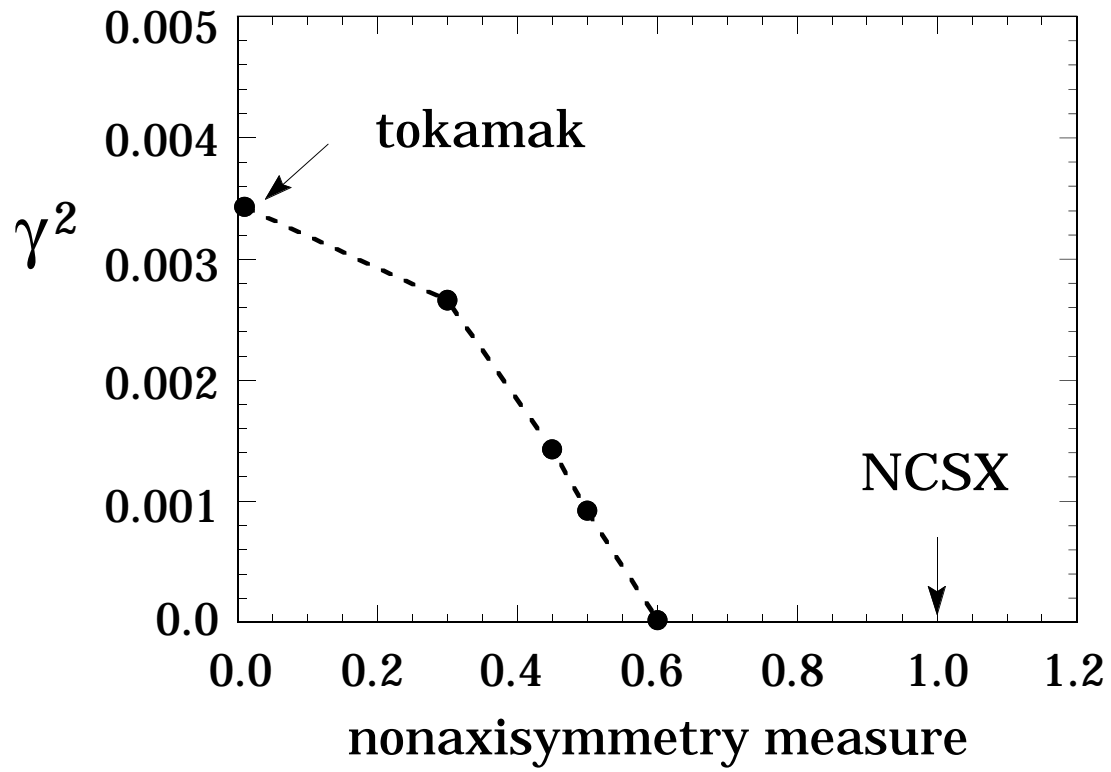


Figure 6:

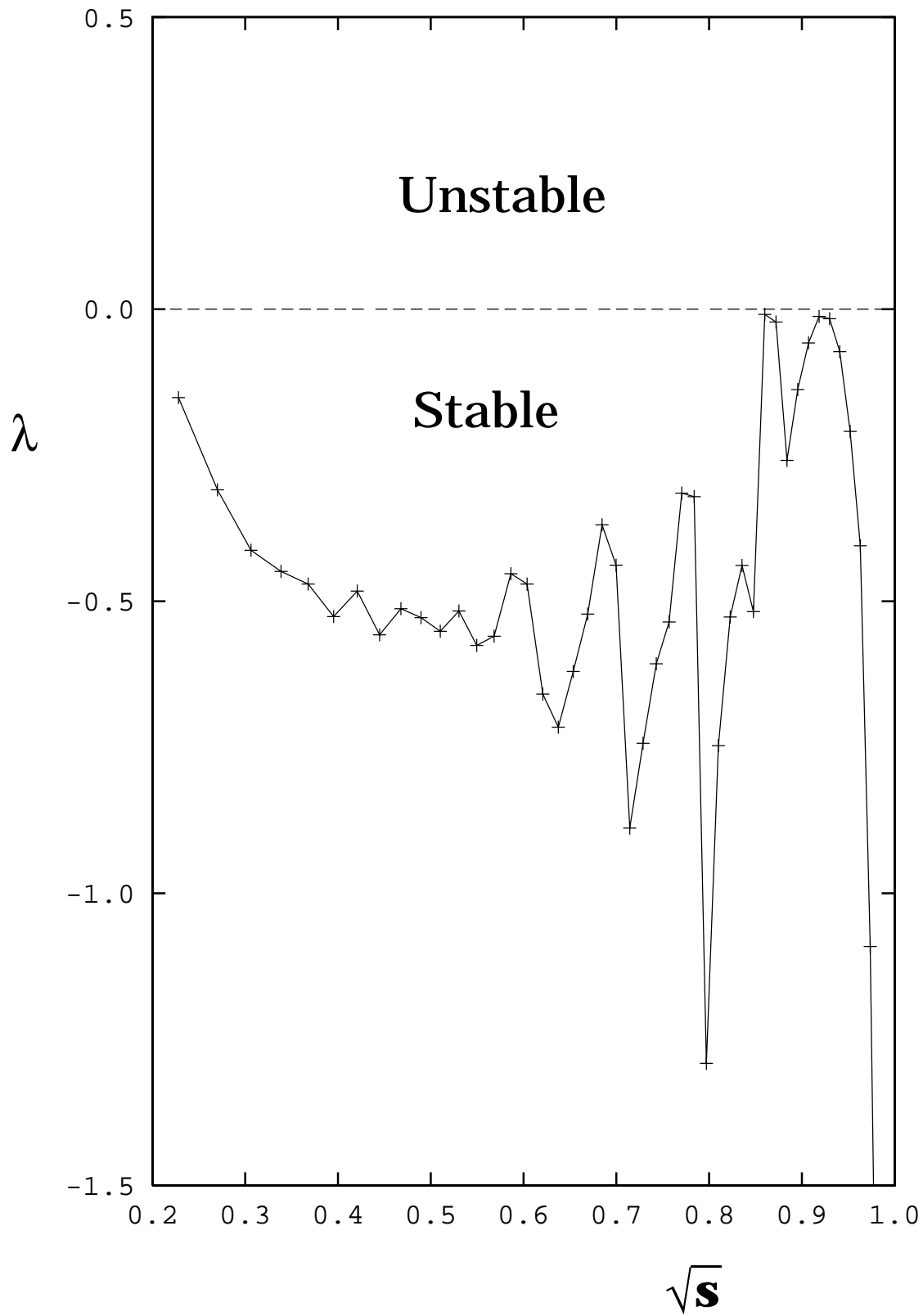


Figure 7: